NONLINEAR MODELLING IN AIRBORNE SIMULATIONS

J.-Michael Bauschat

Institut für Flugmechanik
Deutsche Forschungsanstalt für Luft- und Raumfahrt e.V. (DLR)
Postfach 3267
D-3300 Braunschweig
Federal Republic of Germany

Abstract

The in-flight simulation technique, which is implemented on the DLR research aircraft ATTAS (Advanced Technologies Testing Aircraft System) will be presented. After this brief overview, two particular developments will be discussed in detail. One is a nonlinear 6-degrees-of-freedom real-time aircraft model for the in-flight simulation, the other is a quasi-nonlinear feedforward controller in the ATTAS model following system. Both systems have been investigated in flight-tests, where a typical wide-body transport aircraft has been simulated. Some selected flight-test results will be given, which show the high quality of the developed model following system during nonlinear simulation tasks. The research aircraft and the ATTAS ground-based simulator will be presented briefly.

1. List Of Symbols

$\underline{A}$	system dynamics matrix	α	angle of attack
$\underline{B}$	control input matrix	β	angle of sideslip
H	altitude	γ	climb angle
q	pitch rate or quaternion	Δ	difference or error
r	yaw rate	ε	trim setting
t	time	ζ	rudder angle
$\underline{u}$	control input vector	η	elevator angle or control deflection in the longitudinal motion
V	speed	Θ	pitch angle
u,v,w	components of V	ξ	aileron angle
$\underline{x}$	state vector	Φ	bank angle

Subscripts		Superscripts	
a	aerodynamic axes	*	pseudoinverse of a matrix
E	Error	T	transpose of a matrix
FCU	Fuel Control Unit	-1	inverse of a square matrix
g	earth fixed axis	Ref	trimmed flight state
H	Host aircraft		
I	integral feedback		
l	linear		
M	model aircraft		
nl	nonlinear		
P	proportional feedback		
V	feedforward control		

2. Introduction

The use of extensive system-technique in *state of the art* transport aircrafts is no longer a fact which is under discussion. One item making the Airbus A320 a successful product is its fly-by-wire capability in combination with know-how concerning modern aircraft (a/c) systems. Developments in the near future will bring high augmented transport aircrafts or hypersonic aircrafts with no natural stability.

The disadvantage of all these tendencies is the increasing system complexity. Independent of the complexity the designers have to guarantee the safety of the vehicle before the first flight. A straight answer to the question on how to ensure a proper design, is an extended use of simulation techniques.

Investigations which have been carried out show that not all problems can be solved using ground-based simulators. Phenomena like pilot-induced oscillation (PIO) often only occur, when the pilot is in high-stress situation. During the approach and landing flight testing of the space shuttle for instance, a tendency for PIO was observed during the landing phase. To improve the approach and landing characteristics an adaptive stick-gain was developed ([10]). Testing this filter on fixed-base and moving-base simulators was proved to be inadequate. Flight-tests with the Total In-Flight Simulator (TIFS) of Calspan were necessary.

In the space shuttle program another in-flight simulator is in use. It is the Space Shuttle Training Aircraft (STA) based on a Gulfstream II. The pilots of the orbiters have to train the steep approach and the landing procedure more than 500 times on the STA, before they are qualified to fly it.

The above illustrated strategies developing and testing the flight control system of the shuttle orbiter and the required expenditure to train its crew are aspects, which have to be taken into account in the research concerning augmented future transport aircrafts. Flight simulation under real environmental conditions seems to be a must for those projects.

This paper deals with new models and their applications

in the in-flight simulation of the flying test-bed ATTAS.

3. Principle of In-Flight Simulation

The aim of in-flight simulation is to imprint the characteristics of a vehicle to be simulated on a host a/c. Figure 1 gives a survey of this particular technique.

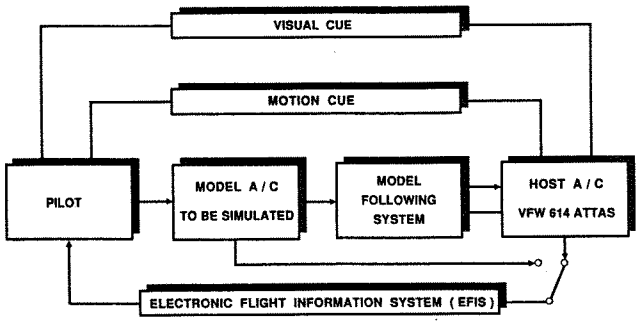

Figure 1. Rough Structure of ATTAS In-Flight Simulation

First of all a brief discription of the main components will be given:

- Pilot

  He has to perform the prepared simulation tasks, which depend for instance on the scientific work to be done. Simulating the automatized flight of an a/c the pilot would be replaced by a digital flight control system. In this case he would have the task to observe the simulated flight.

- Model a/c to be simulated

  In the discussed system this part contains the algorithms which are needed to simulate a nonlinear model a/c under real-time conditions.

- Model following system (MFS)

  It consists of a combination of feedforward and feedback control laws:

  Feedforward control

  These gain matrices compute the control deflections which are required for model following. This part represents the inverse of the host a/c.

  Feedback control

  The feedback gain matrices ensure rapid and gradual decaying error dynamics. One can arrive at this error by substracting selected model outputs from the host outputs. The classical controller includes proportional and integral (PI) gain matrices.

  A requirement of this particular MFS is, it should be independent of the model a/c to be simulated. The advantages under flight-testing aspects are evident.

- Host a/c

  The essential part of the in-flight simulation is an adequate flying test-bed. It must be equipped with a fly-by-wire control system. A data acquisition and recording system must be available.

The principle is as follows:

The pilot has direct control of the computed nonlinear model with his inputs. It is the identical technique, which can be found in ground-based simulation. In an explicit model following the idea is to make selected model states and their changes due to time available to the MFS. The computed outputs from the MFS are inputs to the actuators of the host a/c. The actuators effect the required deflections of the control surfaces (elevator, direct lift control (DLC) flaps, aileron, rudder) and the required thrust. Using this simulation technique has the advantage, that the pilot has the real visual cue and the correct motion stimuli of the model a/c (Figure 1).

Information needed by the pilot are attained from an electronic flight information system (EFIS). Depending on the actual experiment selected states of the model a/c, or the host a/c can be displayed. In the following sections the most important components of the nonlinear ATTAS in-flight simulation will be discussed.

4. Nonlinear Real-Time Aircraft Model

In ground-based a/c-simulation the model description is usually based on nonlinear equations. Because of the computer power which is necessary to implement and to run these models, it was not possible to run them in an in-flight simulation. In the last decade the computer capacity increased extremely, while weight and space decreased. Hence, if this computer capacity is available like on ATTAS, one should make the most of the benefits of nonlinear a/c-modelling.

At the DLR a nonlinear 6-degrees-of-freedom (6-DOF) real-time model a/c was developed ([4]). Some of the focal points developing it were:

- the real-time aspect

  the model and the model-following-system should be computed with a cycle rate of 40 Hz.

- the flexibility

  changing the model to be simulated or the model-characteristics should be easy.

The whole software system can be subdivided into four essential modules:

Module 1 - Initialisation

This module has to be computed first before any other part of the program-system is started. Each model to be simulated has specific parameters which are set here. The nonlinear aerodynamic needs an initialisation as well as the simulation software system itself.

Module 2 - A/C model trim algorithm

The number of initial values which have to be iterated is given by the number of differential equations describing the model. A 6-DOF simulation-model needs six initial values. In this case flight states are given and control states have to be iterated. These are

- elevator angle η
- rudder angle ζ
- aileron angle ξ
- power setting η_{FCU}

- angle of attack α
- bank angle Φ

To get these states a NEWTON-iteration-algorithm is in use, because it converges very fast. The speed aspect is very important with regard to the in-flight simulation application. A trim-phase that lasts too long may result in a big difference between the states of model- and host a/c, when the real-time simulation starts. The algorithm gets the needed flight states from the host a/c.

In a flight-test the simulation pilot, sitting on the left hand side (Figure 2), first has to take over the control of the airborne host a/c.

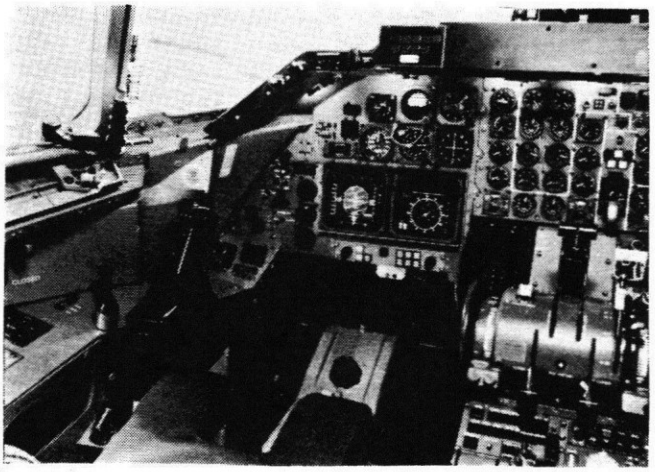

Figure 2. Left Hand Side of the ATTAS-Cockpit

Hence, he has to change the flight-mode from basic to fly-by-wire with the help of an additional input device integrated in the central pedestal. Then he has to establish stationary flight conditions of the host a/c. A so-called *SIM-button* is part of the above mentioned input device. Pressing it, he changes the flight mode from fly-by-wire (host a/c) to simulation (model a/c) and fly-by-wire. Now the trim algorithm in the experimental and control computer of ATTAS starts. During the model trim-phase the pilot gets intermittent information on one of his CRTs not to give any control inputs. How satisfying the trim algorithm works is illustrated in Figure 3, where the time between switching into SIM-mode and trimmed elevator angle η_M is plotted. This particular model a/c was a simulated wide body type a/c comparable with the Airbus A300 and was trimmed in a flight-test.

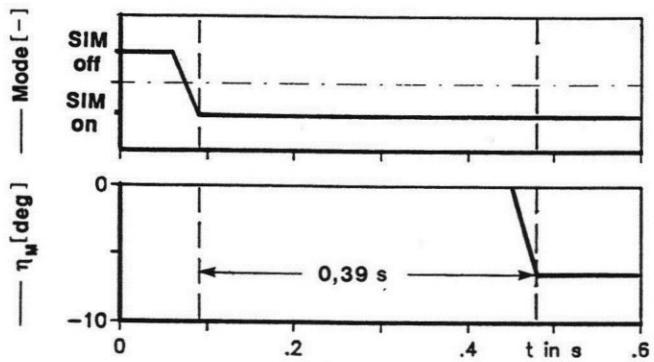

Figure 3. Duration of the 6-DOF Real-Time-Model Trim-Phase (Model A/C: Airbus A300)

Module 3 - Mathematical a/c model and numerical integration

The mathematical description of a typical a/c is given by twelve ordinary differential equations, thirteen if the EULER-angles are computed using a quaternion-algorithm ([9], [4], [13]). With the equations of motion one gets:

- three linear accelerations $\dot{u}_{Kf}$, $\dot{v}_{Kf}$, $\dot{w}_{Kf}$
- three angular accelerations $\dot{p}$, $\dot{q}$, $\dot{r}$
- four quaternions $\dot{q}_0$, $\dot{q}_1$, $\dot{q}_2$, $\dot{q}_3$
- three velocity components of the centre of gravity $\dot{x}_g$, $\dot{y}_g$, $\dot{z}_g$

Taking the real-time aspect into account, a fast numerical integration algorithm is required. Two methods are in use

EULER

The integral is approximated by rectangles

$$y_{t+\Delta t} = y_t + \Delta t \cdot y'_t \tag{1}$$

Compared with the exact solution, the occurring error of the numerical integration increases with $(\Delta t)^2$ ([4]).

ADAMS-BASHFORTH 2nd order

This method is an improved approximation of the integral using trapezoids.

$$y_{t+\Delta t} = y_t + \frac{\Delta t}{2}(3y'_t - y'_{t-\Delta t}) \tag{2}$$

The first integration step has to be performed using a method like EULER, because the value $y'_{t-\Delta t}$ must be available.

All selected simulation and flight-test results including the nonlinear model, were made approximating the differential equations with the ADAMS-BASHFORTH-algorithm.

The model aerodynamic consists of measured and identified data. One obtains the nonlinear derivatives using a high speed table look up method ([7]). An example indicates the quality of the chosen algorithm.

> The nonlinear aerodynamic of the Airbus A300-model (66 2D-tables, 19 1D-tables) needs 9.6 ms in one simulation-cycle on the ATTAS experiment-computer.

The engine model which is in use in this model a/c is a simple 1st order attempt. A more sophisticated one will be implemented as soon as possible.

Module 4 - Computed Model Disturbances

The possibility to disturb the model has several advantages. In the validation-phase for instance, one gets data which are easy to reproduce after every development step. There are two forms to be distinguished

- internal disturbances (pulse-type, 3211, sweep, etc.)
- external disturbances (gust, turbulence, wind)

Both are in use and have been very helpful in testing the model in the ATTAS ground-based simulation and in flight-tests.

5. Model Following System

A lot of work has been done in the last decades concerning model following. Discussing the problem to control airborne vehicles in an in-flight simulation, the reduction in a single-input, single-output system is impossible in most areas of interest. Some very fruitful solutions were published and used in flight-tests based on the theory of small pertubations (e.g. [8], [6]). They controlled the nonlinear plant using the following approaches:

- a linear model of the a/c to be simulated
- a linear open loop control configuration
- techniques to get linear feedback control structures based on analog computation experiences

The benefits of these linear models are e.g.:

- they are easy to handle
- they do not need a large computer capacity
- it is efficient to use them in a linear control-system

It was mentioned in section 2, that the in-flight simulation will be a unique tool investigating the flight mechanics of future aircrafts. Their trajectories which have to be simulated cover several operation points. In this case there is not only the problem of controlling a highly nonlinear plant, the additional problems are

- to simulate a high augmented model a/c
- *nonlinear* piloted simulation tasks have to be taken into account

A new approach has been developed at the DLR, which concentrates upon the *open loop problem*. It will be dicussed in the next section.

5.1 Quasi-Nonlinear Feedforward Controller

This part of the MFS represents, as mentioned above, the inverse model of the host. The difficulty is, that the nonlinear differential equations describing the dynamic of a system cannot be inverted in general.

One solution is discussed in [11], where a forward feeding system is presented, which is a nonlinear quasistationary inverse of the longitudinal a/c motion. This system was designed to follow steady and flyable time functions of commanded altitude and airspeed. It was used e.g. to perform automatic landings.

Another way was chosen for the ATTAS MFS. It is based on the linear, constant coefficient dynamical equations:

$$\dot{\underline{x}} = \underline{\underline{A}} \cdot \underline{x} + \underline{\underline{B}} \cdot \underline{u} \tag{3}$$

with (3) one arrives at

$$\underline{u}_V = \underline{\underline{B}}^{*} (\dot{\underline{x}}_M - \underline{\underline{A}} \cdot \underline{x}_M) \tag{4}$$

which is a linear attempt for a predefined operation point. In the longitudinal motion one have n flight states ($\underline{x}(t)$ is of dimension of n) and m degrees of freedom ($\underline{u}(t)$ is of dimension of m). Therefore the control input matrix $\underline{\underline{B}}$ is not a square matrix and is not invertible. Hence, if n > m, the generalized inverse will yield an exact solution without error ([12]). It is defined by

$$\underline{\underline{B}}^{*} = (\underline{\underline{B}}^{T} \cdot \underline{\underline{B}})^{-1} \underline{\underline{B}}^{T} \tag{5}$$

and is called the *Pseudo-Inverse* of $\underline{\underline{B}}$ ([3], [1]). The necessary and sufficient condition for the existence of a solution is that the pair $\underline{\underline{A}}, \underline{\underline{B}}$ should be controllable.

How easy it is to leave a trimmed operation point and to hurt the implicit given requirement of small pertubations in (4) is illustrated by a simple experiment (Figure 4):

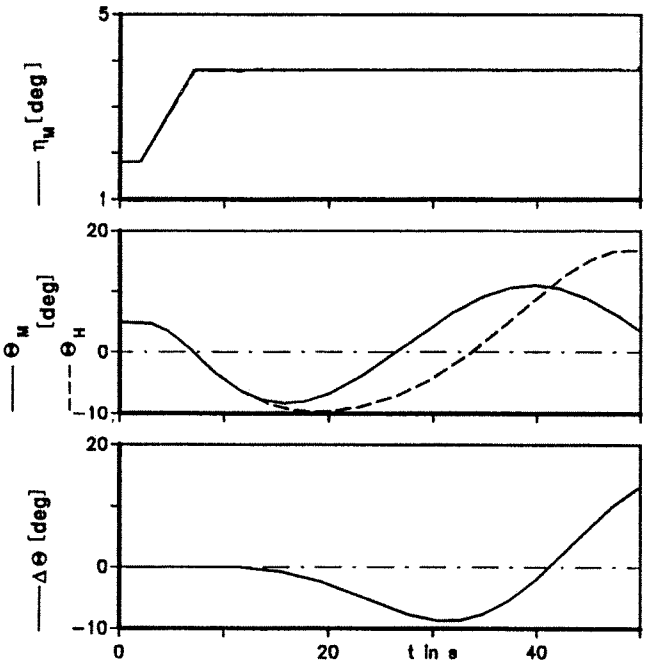

Figure 4. Ramp Input to Modell A/C Elevator (Open Loop - Source: HEUTGER)

A nonlinear model of the VFW 614 was used and its elevator was deflected with a ramp-input and held constant ($\eta_M = 2°$). In this *offline-simulation* the MFS consists only of a feedforward control. The reaction in pitch angle Θ of model and host a/c is just as plotted as the occurring error. The input excites the phugoid motion of the model a/c. Twelve seconds after the ramp input was started an error can be seen and it increases to $\Delta\Theta = 9°$ within 17 seconds. The host a/c cannot follow the model. The idea to improve the linear attempt (4) is quite simple.

> The $\underline{\underline{A}}$ and $\underline{\underline{B}}^{*}$ matrices have to be adapted to the actual operation point.

The developed method is called *Quasi-Nonlinear Feedforward Control* and it is dicussed in great detail in [5]. An abbreviated discription is given here to provide background for the results to be presented.

One gets the $\underline{\underline{A}}$ and the $\underline{\underline{B}}^{*}$ matrix which belong to the actual operation point with the help of the table-look-up method in [7]. The independent variables of the three dimensional (3D) table-look-up are:

- elevator angle η
- trim flap angle ε
- flaps angle η_k

The selected supporting points are listed in Table 1:

η	ε	η_K
− 1,0°	− 6,5°	1,0°
0,0°	− 5,0°	14,0°
1,0°	− 4,0°	
2,0°	− 3,5°	
3,0°	− 3,0°	
4,0°	− 2,6°	
5,0°	− 2,2°	
	− 1,6°	

Table 1. Supporting Points of the 3D Table-Look-Up (source: HEUTGER)

Multiplying the number of points in each group one arrives at 112 combinations. A nonlinear offline simulation program was used to get the trimmed flight-states of the host a/c for each of the given combinations. Using these results, it is possible to compute 3D-tables of the reference-states and the $\underline{\underline{A}}$ and $\underline{\underline{B}}^*$ matrices. The algorithm illustrates Figure 5.

The inputs are the model a/c states $\underline{x}_M(t)$ and their changes due to time $\dot{\underline{x}}_M(t)$. The host a/c control quantities $\underline{u}_H(t)$ and the mentioned 3D-tables.

First a low pass filtering of the host a/c elevator angle η_H must be computed. The short term model following quality of the quasi-nonlinear approach was found not to be as good as the performance of the linear one. This disadvantage is based on the fact that the reaction of a given transport a/c to an elevator input is quite slow. The worst case is a step input to the elevator of the model a/c, which would lead to a very fast reaction of the host aircrafts elevator. However, η_H is one of the independent variables interpolating the matrices $\underline{\underline{A}}$ and $\underline{\underline{B}}^*$. Hence, the dynamic characteristic of (4) changes faster than the one of the system to be controlled. The most dominant self-movement is in this case the phugoid-oscillation and it is the phugoid-time constant, which was used to filter η_H.

In the next part of the algorithm (Figure 5) the values of $\underline{\underline{A}}_I$, $\underline{\underline{B}}_I^*$ and $\underline{x}_{H,I}^{Ref}$ have to be computed.

In the following branch two cases have to be distinguished:

- first computation of the algorithm (initial step)
- the simulation has started

In the first case the errors between model a/c states and interpolated host a/c states must be known. This systematic error of the model would induce an output of the feedforward controller without a change in the model a/c states. Otherwise the actual difference between model a/c and interpolated host a/c states have to be computed. These differences are the inputs to the *adapted, linear* open-loop equations (4).

The improvement may illustrate the example given in Figure 4. Again the ramp-input was used in order to deflect the elevator of the model a/c in an *offline-simulation*. But this time the open-loop is the quasi-nonlinear one (Figure 6):

Quasi - Nonlinear Feedforward Control Of The Longitudinal Motion

Input : Model a / c states $\underline{x}_M = [V_{AM}, \alpha_M, \Theta_M, q_M] \quad \dot{\underline{x}}_M = [\dot{V}_{AM}, \dot{\alpha}_M, \dot{\Theta}_M, \dot{q}_M]$

Host a / c control quantities $\underline{u}_H = [\eta_H, \eta_{KH}, \varepsilon_H]$

Set of tables with A and B* - matrices for selected trim states $\underline{x}_H$

Output : Feedforward control outputs $\Delta\underline{u}_{V,qnl} = [\Delta\eta_V, \Delta\eta_{DLC,V}, \Delta\eta_{FCU,V}]$

Low pass filtering of the host a / c elevator angle $\eta_H \qquad \eta_{HLP} \leftarrow f(\eta_H, T_{Phugoid})$

High speed table look up interpolates :

$\underline{\underline{A}}_I = f(\eta_{HLP}, \eta_{KH}, \varepsilon_H) \quad \underline{\underline{B}}_I^* = f(\eta_{HLP}, \eta_{KH}, \varepsilon_H) \quad \underline{x}_{H,I}^{Ref} = f(\eta_{HLP}, \eta_{KH}, \varepsilon_H)$

Initial step ($t_{sim} = 0 - \Delta t$)

yes

Errors between host and model a/c states

$\Delta\underline{x}_E \leftarrow \underline{x}_M - \underline{x}_{H,I}^{Ref}$

no

Differences between host and model a / c states : $\Delta\underline{x}_M(t) \leftarrow \underline{x}_M(t) - \underline{x}_{H,I}^{Ref}(t)$

Feedforward control outputs : $\underline{u}_{V,qnl} \leftarrow \underline{\underline{B}}_I^* [\dot{\underline{x}}_M(t) - \underline{\underline{A}}_I (\Delta\underline{x}_M(t) - \Delta\underline{x}_E)]$

Figure 5. Algorithm of the Quasi-Nonlinear Feedforward Control

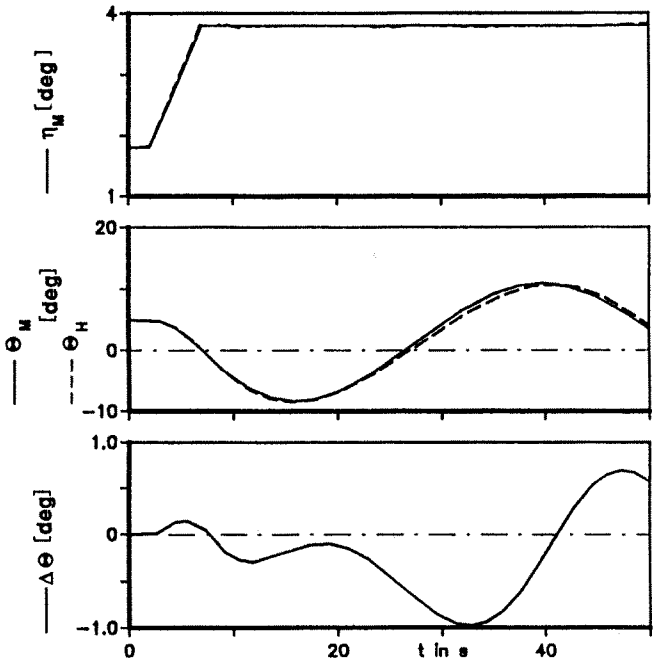

Figure 6. Ramp Input to Model A/C Elevator (Quasi-Nonlinear Feedforward Control - Source: HEUTGER)

It is obvious that the occurring error in pitch between model and host a/c is small and good model-following can be achieved without feedback control. Some experiences using this approach in flight-tests will be given in one of the following sections.

5.2 Feedback Controller

The feedback gains, which are in use in the MFS on ATTAS, were computed using an interactive computer-aided-design technique ([3]). Figure 7 illustrates the structure of the controller:

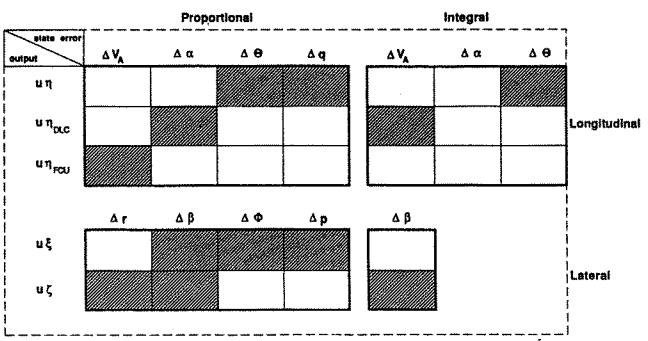

Figure 7. Structure of the ATTAS Feedback Contoller (Source: HENSCHEL)

The design-aim is to reduce errors which are caused by effects like ([3]):

- Modelling errors
- External disturbances
- Actuator non-linearities and time delays
- Sensor bias and time delays

Equation (6) illustrates that the state error vector $\Delta \underline{x}_E(t)$ (including changes due to time) represents the differences between host a/c and model a/c states:

$$\Delta \underline{x}_E(t) = \underline{x}_H(t) - \underline{x}_M(t) \qquad (6)$$

$\Delta \underline{x}_E(t)$ has to be minimized with the feedback controller given in Figure 7. Hence, it is most important to get the the exact values of $\Delta \underline{x}_E(t)$. Figure 8 shows the characteristic of the source of the host a/c flight-states:

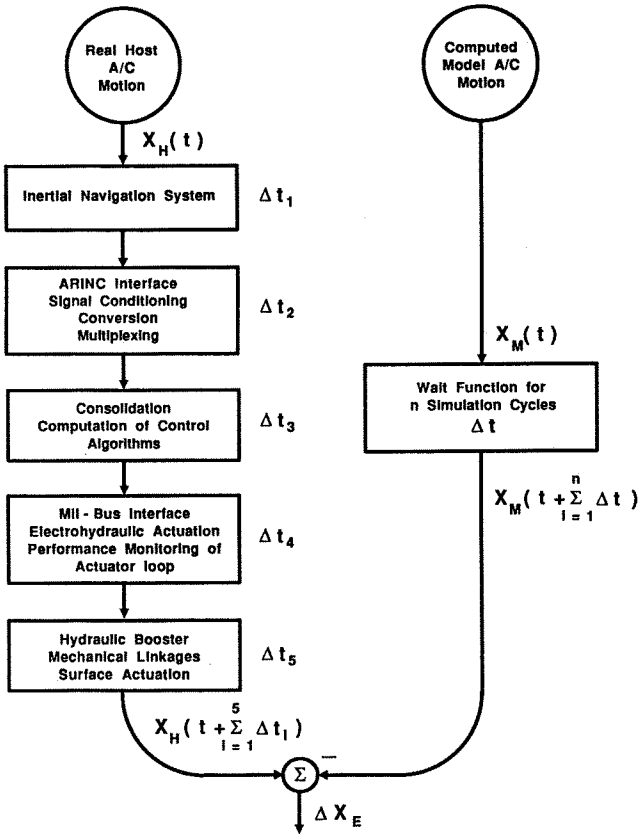

Figure 8. Signal Source Characterisitic of Host and Model A/C

It can be seen that several *real world effects* have to be taken into account. Some significant contributions to an effective time delay come from e.g.:

- the measurement system
- the interfacing
- the actuator dynamic
- the reaction of the host a/c

In Figure 8 they are listed in greater detail.

A simple solution to get a comparable model state is to delay it. The particular time delay which has to be used is an identification result of the signal source of the host a/c.

In the flight-tests performed this technique has been used.

6. Advanced Technologies Testing Aircraft System (ATTAS)

The concept of ATTAS consists of two parts

- ATTAS in-flight simulator
- ATTAS ground based simulator

Every scientific development on ATTAS is a result of interaction between these essential elements.

6.1 ATTAS In-Flight Simulator

ATTAS is based on a VFW 614, twin-turbofan, short-haul 44-passengers a/c (Figure 9).

Figure 9. DLR In-Flight Simulator VFW 614 ATTAS

The VFW 614 is ideally suited as a general purpose test-bed due to the size, cabin space, loading capacity and flight performance. With full fuel, about 3.5 tons of test equipment can be loaded. The flight perfomance with cruising altitude of 30 000 ft, maximum cruising speed of 285 kts CAS and a rather low landing speed of about 100 kts is adequate for a large transport a/c flight regime representation. Figure 10 illustrates the ATTAS-flight envelope:

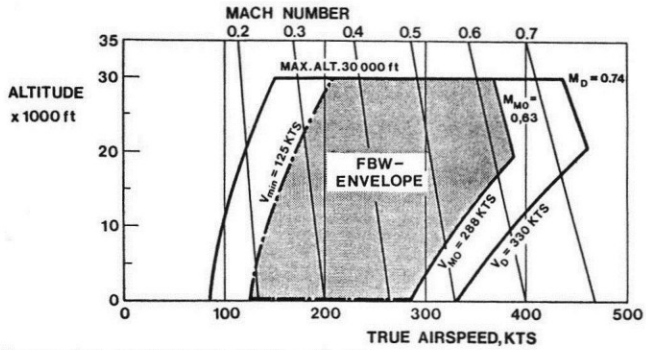

Figure 10. ATTAS-Flight Envelope

In-flight simulation is an important application but not the only one. Some other research areas are:

- Flight Control - Active Control
- Flight Guidance - Air Traffic Control
- Future Cockpit
- Fly-By-Wire/Light Control System

The heart of ATTAS is the fly-by-wire/light system. It is up to the present based on a five computer system ([2]). The ATTAS-dual-redundant fly-by-wire flight-control-system is beeing developed. It will give the a/c the important touch-down capability. In addition to the usual control surfaces it is equipped with six direct lift control flaps (DLC's, three on each wing). With these DLC-flaps ATTAS is a 5-DOF in-flight simulator.

6.2 ATTAS Ground-Based Simulator

The real-time simulation of ATTAS on ground is an important tool. It simulates the a/c as well as making it possible to do without motion cue and a visual system. The Mil-Spec on-board computers are substituted by commercial Data General systems. An original ATTAS-cockpit belongs to the simulator (Figure 11).

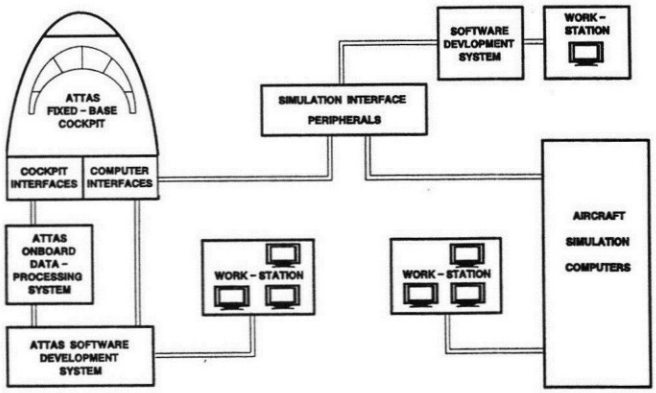

Figure 11. ATTAS Groundbased Simulation Facilities

Every experiment flown on the in-flight simulator can be checked on the ground. The scientist is able to validate his software and obtain first results. Another important fact is to train the pilots and get their comments before being airborne. The ground simulation reduces the costs and also a lot of development risks. The high standard of the ATTAS ground based real-time simulator allows the realization of typical experiments concerning simulation technique.

7. Flight-Test Results

The quasi-nonlinear model following system and the nonlinear 6-DOF real-time model a/c were first tested together in the ATTAS ground-based simulator. The results were very promising. After this test phase on ground, the whole system was flight-tested on ATTAS. All results which will be presented were simulations of a wide body transport a/c (2 engines, 115 tons).

Figure 12 presents some flight states, which were achieved while the elevator of the model a/c was deflected by a computed sweep input. It started with 0.01 Hz and ended after 120 seconds with 1 Hz. In the Figure one phugoid oscillation is plotted, which can be seen in the graphs of the true airspeeds $V_{A,M}$ and $V_{A,H}$. The speed error ΔV_A is very small.

A constant offset exists between the two curves of α_M and α_H. This error occurs between some particluar flight states of model and host a/c, like e.g. angle of attack, pitch angle and bank angle. The reason for this effect is, that after the nonlinear model a/c is trimmed, its flight states differ from the states of the host a/c. This offset is computed and used as a constant during the whole simulation. Hence, it will not be minimized by the model following system. Relative to the angle of attack in Figure 12 this offset has a value of 1.6 degrees. The curve of $\Delta\alpha$ illustrates that the additional error between α_M and α_H is minimal. Also the error between the pitch rates is acceptable.

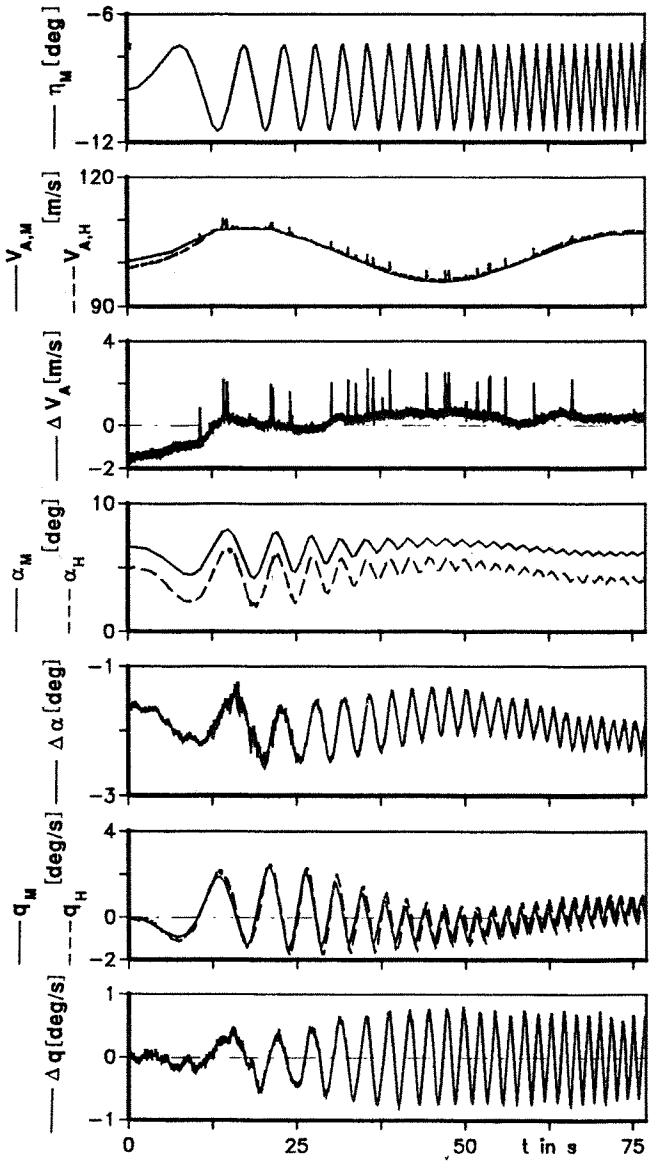

Figure 12. Sweep Input to the Elevator of the Model A/C

One of the piloted tasks which were performed shows Figure 13:

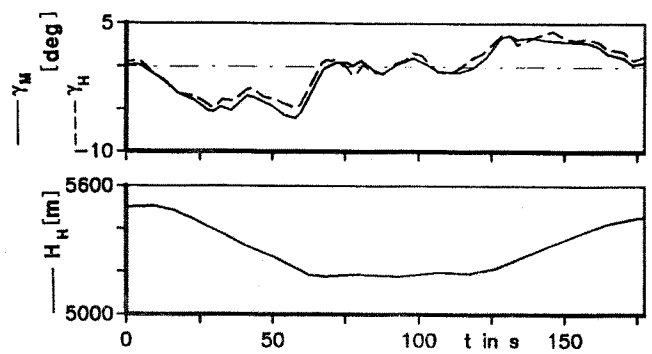

Figure 13. Climb Angles and Altitude

The pilot had to fly some flight level changes and two of them are plotted. A subdivision of the illustrated task into three parts is possible. First a descent from roughly 5500m down to 5200m was flown (part 1). He had to establish stationary flight conditions. In this second part the two climb angles γ_M and γ_H are approximately zero. In the third part the a/c climbed back to 5500m.

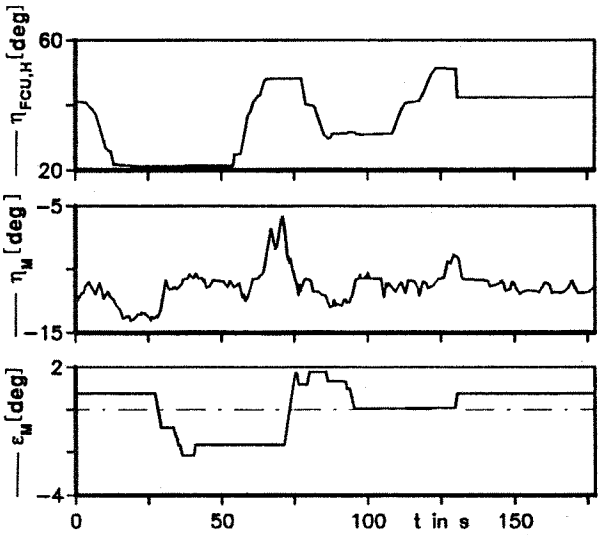

Figure 14. Commanded Thrust Setting, Elevator Angle and Trim Setting

Figure 14 shows that the descent was flown with a very low commanded thrust. To achieve a climb angle $\gamma = 0$, the pilot increased the thrust setting from 35% to 81%. This effected a *nose up* of the simulated Airbus-type, which he had to compensate with a positive elevator input by pushing the stick. The same effect can be observed, when he began the climb.

The chosen trim-setting indicates the angle ε_M. It can be seen, that the pilot changed the trim state of the a/c at the beginning of every new part. That means the non-linear model a/c was flown in different operation points and so the task can be called *nonlinear.*

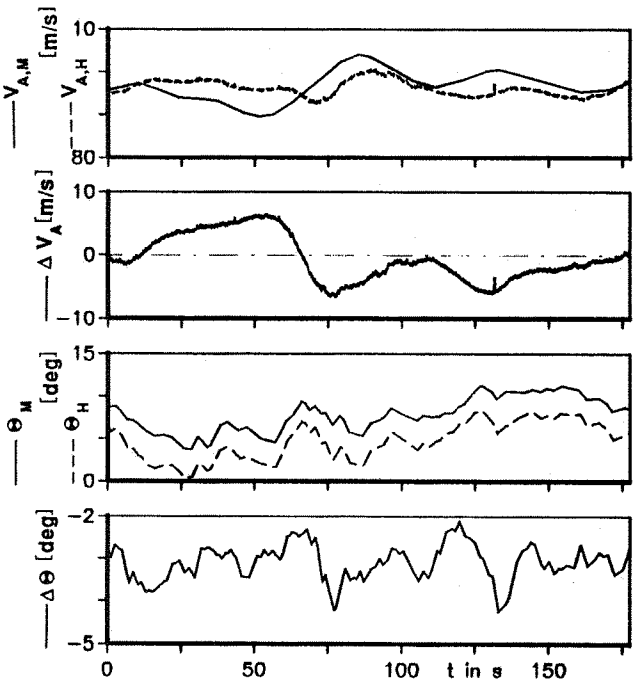

Figure 15. Flight States of Model and Host A/C

In Figure 15 the speed curve shows, that the model a/c was approximately 5 m/s slower than the host a/c. In the beginning of part 2 and part 3 of the mission, while the thrust-setting η_{FCU} increased, the model a/c was faster. The reason for this error seems to be the simple 1st order engine model. During the descent (part 1) and the beginning of the two other parts, the behaviour of the engine model attempt results in model a/c states which

are not realistic. Between the pitch angles Θ_M and Θ_H the above mentioned offset can be seen ($\Theta_{offset} \sim 3°$). The effective error is between $+/-1°$ and is absolutely acceptable.

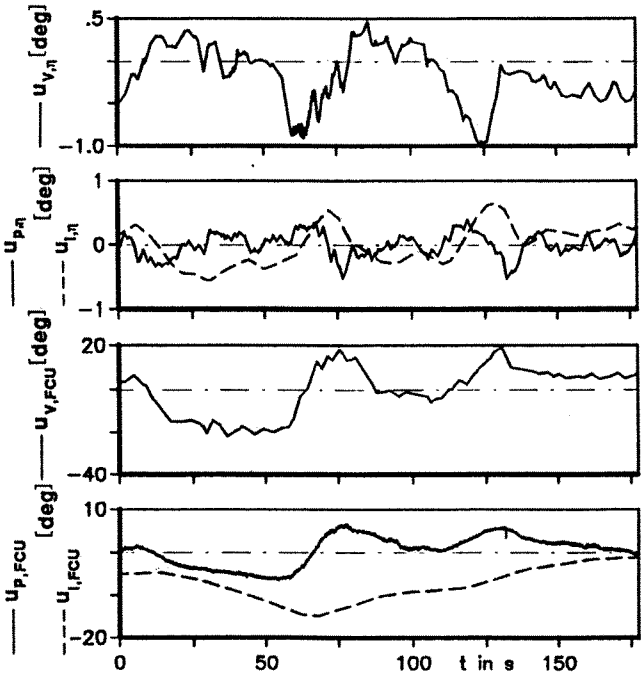

Figure 16. Model Following System Outputs

Figure 16 illustrates the MFS outputs to elevator and FCU of the host a/c. The above described nose up effect as consequence of the quite rapidly increasing power setting is simulated by the feedforward control output to the elevator ($u_{V,\eta}$). It commands a negative elevator deflection, which means pulling the stick, because increasing the thrust causes *nose down* on the VFW 614. This a/c has the engines above the wings. The feedforward control output to the FCU is comparable with the commanded thrust (Figure 14). It can be seen how the integral feedback control output $u_{I,FCU}$ decreases during the first 70 seconds. The engines of the host a/c cannot support the decreasing speed required by the model a/c.

The model following in the lateral motion was investigated performing a special flight task. The pilot flew a turn reversal, which is shown in Figure 17.

The activity of the pilot shows the curves of model aileron ξ_M and inner model aileron $\xi_{M,i}$ deflection of the left wing. The constant offsets between the bank angles Φ_M and Φ_H and the yaw rates r_M and r_H indicate that the two flight states Φ_H and r_H of the host a/c were not zero when the pilot started the model a/c trim algorithm. This Figure illustrates the high model following quality in the lateral motion, because the effective error is very small.

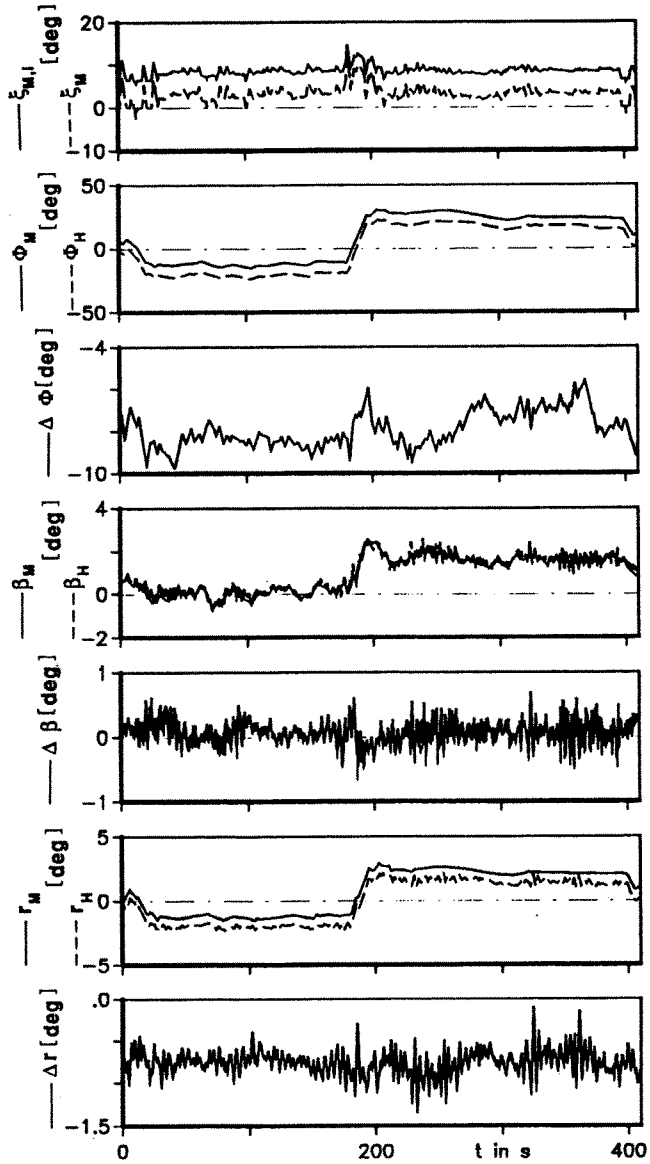

Figure 17. In-Flight Simulation Results of a Turn Reversal

8. Conclusions

The nonlinear in-flight simulation technique, developed at the Institute for Flight Mechanics of the German Aeronautical Research Establishment (DLR), could be presented. After its implementation on the flying test-bed, ATTAS, several flight-tests have been performed, where a typical wide body transport a/c was simulated. The achieved model following performance proved to be excellent. The advantage is, that typical *nonlinear influences* like:

- changing the configuration of the model a/c (flaps, slats, etc.)
- changing in the deflections of trim surfaces
- large speed variations

can be simulated in flight as long as the given flight envelope of the host a/c is not violated.

Some necessary improvements of the existing in-flight simulation system will be:

- **the engine and thrust model of the 6-DOF real-time model a/c must be more realistic.**
- **the trim algorithm should compute a flight state of model and host a/c with an identical pitch angel, or an identical offset between both after each trim phase. Θ gives the pilot significant information about the longitudinal motion of the a/c. That means, it is an error sensitive parameter in the in-flight simulation.**

9. References

[1] HAMEL, P.G. *Techniques For Model Identification And Design Of Model Following Control Systems* International Symposium on Stability, Academy National de l'Air et de l'Espace / ONERA, Paris, 3.-5. Nov. 1987

[2] HANKE, D. - BOUWER, G. *DFVLR In-Flight Simulators ATTAS and ATHeS for Flying Qualities and Flight Control Research* AGARD Conference Proceedings No. 408, Flight Simulation, FMP Symposium, Cambridge, 1985

[3] HENSCHEL, F. - CHETTY, S. *An Improved Design Technique for Model Following Control Systems In 'In-flight Simulation'* DFVLR Forschungsbericht FB 87-09, Braunschweig, Februar 1987

[4] HEUTGER, H. - BAUSCHAT, J.-M. - HEINTSCH, T. *Entwicklung eines nichtlinearen Flugzeugsimulations-Programms für die In-Flight-Simulation mit dem Flugversuchsträger VFW 614-ATTAS* DLR Institutsbericht IB 111-89/21, Braunschweig, Juli 1989

[5] HEUTGER, H. - BAUSCHAT, J.-M. - HAHN, K.U. *Entwicklung eines Vorsteuerungsansatzes zur Erweiterung der Flugenveloppe der In-Flight-Simulation mit dem Flugversuchsträger ATTAS* DLR Institutsbericht IB 111-90/06, Braunschweig, Februar 1990

[6] LANGE, H.-H. *Flugerprobung des Modellfolgereglers für die HFB 320 zur Simulation des Airbus A310 im Fluge* DFVLR Mitteilung 79-13, Braunschweig, September 1979

[7] MÜLLER, B. *Ein optimierter Tabellen-Interpolationsalgorithmus für die Echtzeitanwendung* DLR Institutsbericht IB 111-90/05, Braunschweig, 1990

[8] MOTYKA, P.R. - RYNASKI, E.G. - REYNOLDS, P.A. *Theory and Flight Verification of the TIFS Model-Following System* Journal of Aircraft, Vol. 9, No. 5, May 1972

[9] NIEMZ,W. *Anwendung der Quaternionen auf die allgemeinen Bewegungsgleichungen der Flugmechanik* Zeitschrift für Flugwissenschaften 11 (1963), Heft 9

[10] POWERS, B.G. *An Adaptive Stick-Gain to Reduce Pilot-Induced Oscillation Tendencies* Journal of Guidance, Control and Dynamics, Vol. 5, March-April 1982

[11] REDEKER, A. *Beiträge zur Verbesserung der Führungsgenauigkeit von Flugreglern* Dissertation an der TU Braunschweig, April 1986

[12] RYNASKI, E. G. *Adaptive multivariable model following (for aircraft control)* Joint Automatic Control Conference, San Francisco, August 1980

[13] SALIARIS, C. *Grundlagen der Modellierung von Flächenflugzeugen* DLR Institutsbericht IB 111-87/22, Braunschweig, 1987